

# A numerical method for a transient quantum drift-diffusion model arising in semiconductor devices

Tomoko Shimada · Shinji Odanaka

© Springer Science+Business Media LLC 2008

**Abstract** This paper describes a numerical method for a transient quantum drift-diffusion model arising in semiconductor devices. The discretization method is presented with emphasis on adaptive time discretization. An adaptive time step algorithm is constructed by introducing the derivative of the free energy of the system, which has an essential property to understand the carrier behavior of the time-dependent problems. The algorithm is verified with switching characteristics of one-dimensional n<sup>+</sup>-n-n<sup>+</sup> silicon diodes. It is shown that the time step is adapted to the switching characteristics. The new algorithm significantly reduces the total number of time steps.

**Keywords** Quantum drift-diffusion model · Numerical scheme · Simulation · Partial differential equation · Free energy · Semiconductors

## 1 Introduction

The carrier transport properties in scaled semiconductor devices depend on the quantum mechanical effects even at room temperature (i.e. at high temperature). For the modeling of such semiconductor transport, the quantum drift-diffusion (QDD) model, which is also called the density-gradient model [1], has been introduced as a quantum corrected version of the classical drift-diffusion model with

$O(\hbar^2)$  correction to the stress tensor [1, 2]. This model is suited to incorporate quantum confinement and tunneling effects in scaled semiconductor devices [3, 4]. The numerical method for the QDD model is a major concern to understand such physical phenomena and to predict electrical characteristics for scaled semiconductor devices. Several studies have proposed numerical methods for the stationary QDD models, including positivity-preserving iterative methods [5–7], high-accuracy nonlinear schemes [6, 8], and a high-resolution method for quantum confinement simulations [9]. Only some results on numerical methods for the transient QDD model are available [10].

This paper describes a numerical method for a transient quantum drift-diffusion model with emphasis on adaptive time discretization. The adaptive time step algorithm is proposed by introducing the derivative of the free energy of the system. The outline of the paper is as follows: Sect. 2 describes a time-dependent quantum drift-diffusion model. In Sect. 3, the derivative of the free energy for the QDD system is introduced. Section 4 describes discretization and an iterative solution method. Space discretization presented in [6] is applied. In Sect. 5, we construct an algorithm of adaptive time step control using the derivative of the free energy of the system. In Sect. 6, the resulting algorithm is validated for the switching characteristics of one-dimensional n<sup>+</sup>-n-n<sup>+</sup> silicon diodes.

## 2 A time-dependent quantum drift-diffusion model

The QDD equation is derived from a Chapman-Enskog expansion of the Wigner-Boltzmann equation adding a collision term [1, 2]. The QDD model is introduced as a quantum-corrected version of the classical DD model with

T. Shimada (✉)  
Graduate School of Information Science and Technology, Osaka University, Toyonaka, Osaka, 560-0043, Japan  
e-mail: t-shimada@ist.osaka-u.ac.jp

S. Odanaka  
Cybermedia Center, Osaka University, Toyonaka, Osaka, 560-0043, Japan

$O(\hbar^2)$  corrections to the stress tensor [1]. Under the assumption of Boltzmann statistics, the time-dependent QDD model consists of the following system:

$$\varepsilon \Delta \varphi = q(n - p - C), \quad (1)$$

$$n_t = -\frac{1}{q} \operatorname{div} \left( q \mu_n n \nabla \left( \varphi - \frac{kT}{q} \log \left( \frac{n}{n_i} \right) + \gamma_n \right) \right) - r, \quad (2)$$

$$p_t = \frac{1}{q} \operatorname{div} \left( q \mu_p p \nabla \left( \varphi + \frac{kT}{q} \log \left( \frac{p}{n_i} \right) - \gamma_p \right) \right) - r, \quad (3)$$

where  $\varphi$  is the electrostatic potential,  $n$  and  $p$  are the electron and hole densities.  $\varepsilon$  is the electric permittivity,  $q$  is the electronic charge,  $k$  is the Boltzmann's constant,  $T$  is the temperature,  $C$  is the ionized impurity density,  $n_i$  is the intrinsic density, and  $r$  is the recombination term.  $\mu_n$ ,  $\mu_p$  are mobilities of electrons and holes, which are related to the diffusion coefficients by the Einstein's relation as

$$D_n = \frac{kT}{q} \mu_n, \quad D_p = \frac{kT}{q} \mu_p. \quad (4)$$

The quantum potentials  $\gamma_n$ ,  $\gamma_p$  are derived from the  $O(\hbar^2)$  corrections to the stress tensor [1] and the expression for the quantum potentials was written as

$$\gamma_n = 2b_n \frac{\Delta \sqrt{n}}{\sqrt{n}}, \quad \gamma_p = 2b_p \frac{\Delta \sqrt{p}}{\sqrt{p}}. \quad (5)$$

The coefficients for electrons and holes are further identified by

$$b_n = \frac{\hbar^2}{12qm_n^*}, \quad b_p = \frac{\hbar^2}{12qm_p^*}, \quad (6)$$

where  $\hbar$  is the Planck's constant,  $m_n^*$  and  $m_p^*$  are effective masses for the electrons and holes, respectively. It is pointed out that the form of the quantum potentials is different by a factor of 1/3 from the Bohm potential [11].

Assuming Boltzmann statistics, the generalized chemical potentials (the generalized quasi-Fermi level) are introduced as

$$\varphi_n = \varphi - \frac{kT}{q} \log \left( \frac{n}{n_i} \right) + \gamma_n, \quad (7)$$

$$\varphi_p = \varphi + \frac{kT}{q} \log \left( \frac{p}{n_i} \right) - \gamma_p. \quad (8)$$

Then, the electron and hole densities are expressed as

$$n = n_i \exp \left( \frac{q(\varphi + \gamma_n - \varphi_n)}{kT} \right), \quad (9)$$

$$p = n_i \exp \left( \frac{q(\varphi_p + \gamma_p - \varphi)}{kT} \right). \quad (10)$$

Assuming that  $r = 0$  in (3), the fourth-order QDD equation considering only electrons is split into two second order equations [3, 12], by introducing the generalized chemical potentials [13], as follows:

$$n_t = \operatorname{div} J_n, \quad (11)$$

$$J_n = -\mu_n n \nabla \varphi_n = \mu_n \nabla n - \mu_n n \nabla (\varphi + \gamma_n), \quad (12)$$

$$2b_n \nabla^2 S - \gamma_n S = 0 \quad (13)$$

where  $J_n$  is the current density.  $S$  is the root-density  $\sqrt{n}$ . (7) is rewritten as (13) in terms of the variable  $S$ , which requires the positivity of solutions  $S$ . Then (11) and (13) are self-consistently coupled with the Poisson equation,

$$\lambda^2 \Delta \varphi = n - C \quad (14)$$

where  $\lambda$  is the Debye length. All of the potentials are scaled by the Boltzmann voltage  $kT/q$ .

The choice of the unknown variables is an important issue to solve the expanded equation system of the QDD model. Using a new variable

$$u = \frac{\varphi + \gamma_n - \varphi_n}{2}, \quad (15)$$

the root-density is rewritten as

$$S = \sqrt{n} = \sqrt{n_i} \exp \left( \frac{\varphi + \gamma_n - \varphi_n}{2} \right) = \sqrt{n_i} e^u. \quad (16)$$

By employing an exponential transformation of variables  $S = \sqrt{n}$ , (13) is replaced by the equivalent form in terms of the variable  $u$ , i.e.,

$$b_n \nabla \cdot (S \nabla u) - Su = -\frac{S}{2}(\varphi - \varphi_n). \quad (17)$$

Exponential transformations were successfully used in the study of a nonlinear fourth-order parabolic equation [14] and stationary quantum hydrodynamic equations [15]. In the QDD model the exponential transformation allows us to derive (17) from (13) by using (15) [6]. If the variable  $u$  is uniformly bounded, the electron density is maintained to be positive. This leads to a numerical advantage for the iterative solution method of the QDD model [6].

In this paper, we consider a one-dimensional time-dependent QDD model for only electrons in the bounded domain  $\Omega = (0, L)$ ,  $L > 0$ .

$$\lambda^2 \frac{d^2 \varphi}{dx^2} = n - C, \quad (18)$$

$$b_n \frac{d}{dx} \left( S \frac{du}{dx} \right) - Su = -\frac{S}{2}(\varphi - \varphi_n), \quad (19)$$

$$\frac{\partial n}{\partial t} = \frac{\partial}{\partial x} \left( \mu_n \frac{\partial n}{\partial x} - \mu_n n \frac{\partial}{\partial x} (\varphi + \gamma_n) \right). \quad (20)$$

The system is completed by an initial condition

$$n(x, 0) = n_0 \quad \text{in } (0, L), \quad (21)$$

and the boundary conditions, assuming that no quantum effects occur at contacts and hence  $\gamma_n = 0$  at contacts,

$$n(0, t) = n(L, t) = C, \quad (22)$$

$$\varphi(0, t) = \varphi_b, \quad (23)$$

$$\varphi(L, t) = \varphi_b + \varphi_{appl}, \quad (24)$$

$$u(0, t) = u(L, t) = \frac{\varphi_b}{2}, \quad (25)$$

where  $\varphi_{appl}$  is an applied bias voltage.  $\varphi_b$  is the scaled built-in voltage,  $\varphi_b = \log \frac{C}{n_i}$ .

### 3 Free energy form

The free energy of the system has an essential property to understand the asymptotic behavior of the solutions of the time dependent problems. For this reason, the free energy form for the classical drift-diffusion (DD) model was first discussed by Mock [16], and by Gajewski and Gröger under the zero applied bias assumption [17, 18]. The relative free energy of the classical DD model for only electrons under Boltzmann statistics is described as

$$W_{cl} = kT \int_0^L \left( n \left( \log \left( \frac{n}{n^*} \right) - 1 \right) + n^* \right) dx + \frac{\varepsilon}{2} \int_0^L \left| \frac{d}{dx} (\varphi - \varphi^*) \right|^2 dx \quad (26)$$

where  $n^*$  and  $\varphi^*$  are the stationary solutions of the electron density and electrostatic potential, respectively. By a straightforward calculation, we obtain the following form as the derivative of the relative free energy:

$$\frac{dW_{cl}}{dt} = \int_0^L J_n \frac{d}{dx} (\varphi_n - \varphi_n^*) dx \quad (27)$$

where  $\varphi_n^*$  is the stationary generalized chemical potential. Under the zero applied bias assumption,  $n^*$  and  $\varphi^*$  are the thermal equilibrium solutions and hence  $\nabla \varphi_n^* \equiv 0$  in  $(0, L)$ . In this case, assuming that  $r = 0$ , there is the following estimate:

$$\frac{dW_{cl}}{dt} = \int_0^L J_n \frac{d\varphi_n}{dx} dx = \int_0^L -q\mu_n n \left| \frac{d\varphi_n}{dx} \right|^2 dx \leq 0. \quad (28)$$

This means that the relative free energy is a Lyapunov function. Fig. 1 shows a time-dependent behavior of electrons calculated by the classical DD model under the zero applied bias after supplementing an additional electron densities in the channel. As shown in Fig. 2, it is also confirmed from

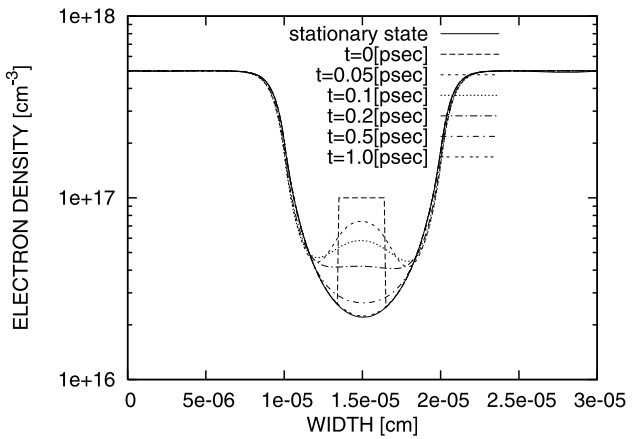


**Fig. 1** Time-dependent behavior of electrons calculated by the classical DD model for an  $n^+$ -n-n $^+$  device with the channel length of  $0.1 \mu\text{m}$

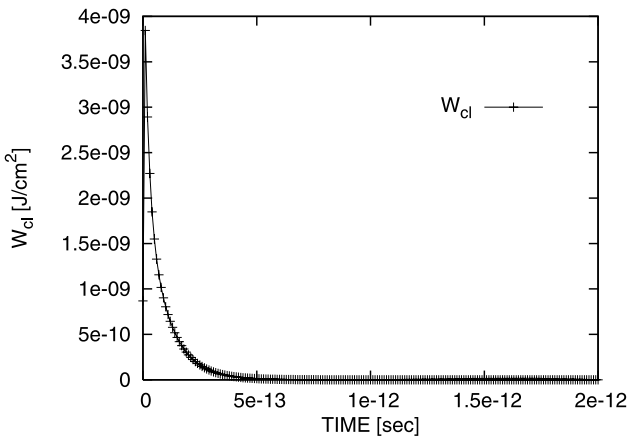


**Fig. 2** Relative free energy as a function of time for the classical DD model

the simulation result that the relative free energy of the system under the zero applied bias is monotonically decreased in time. In a QDD model, a derivative of the relative free energy of the system is introduced to simulate the asymptotic behavior of the numerical solutions to the stationary state [19].

In order to understand the transient behavior of electrons in the more general case, we introduce a non-positive function as a derivative of the free energy of the QDD system. As discussed later, an adaptive time step control for time discretization is designed by predicting the derivative of the free energy of the system. By using the generalized chemical potential, we can define the same form as that of the classical DD model as follows:

$$H(t) = \int_0^L J_n \frac{d\varphi_n}{dx} dx. \quad (29)$$

In [20], under the Dirichlet boundary condition  $\varphi(0) = \varphi(L) = 0$  a free energy form for the QDD model is intro-

duced as

$$\begin{aligned} W_{qm}(n) = & \frac{\hbar^2}{6m_n^*} \int_0^L \left| \frac{d}{dx} \sqrt{n} \right|^2 dx + kT \int_0^L n(\log n - 1) dx \\ & + \frac{\varepsilon}{2} \int_0^L \left| \frac{d\varphi}{dx} \right|^2 dx. \end{aligned} \quad (30)$$

In this case, a straightforward calculation for the derivative of the free energy yields

$$\frac{dW_{qm}}{dt} = \int_0^L J_n \frac{d\varphi_n}{dx} dx. \quad (31)$$

As shown in [20], then, the thermal equilibrium solution is obtained as the state of minimal free energy.

#### 4 Discretization and iterative method

For time discretization we can discretize (20), employing an implicit time discretization. Let  $T > 0$  be given, and the time interval  $[0, T]$  is partitioned into  $N$  subintervals by introducing the temporal mesh  $\{t_k : k = 0, \dots, N\}$ , where  $0 = t_0 < t_1 < \dots < t_N = T$ . Let  $\tau_k = t_k - t_{k-1} > 0$  be the time step. For  $k = 1, \dots, N$ , we obtain the semidiscretization of (18)–(20) in time

$$\lambda^2 \frac{d^2\varphi_k}{dx^2} = n_k - C, \quad (32)$$

$$b_n \frac{d}{dx} \left( S_k \frac{du_k}{dx} \right) - S_k u_k = -\frac{S_k}{2} (\varphi_k - \varphi_{n_k}), \quad (33)$$

$$\frac{1}{\tau_k} (n_k - n_{k-1}) = \frac{\partial}{\partial x} \left( \mu_n \frac{\partial n_k}{\partial x} - \mu_n n_k \frac{\partial}{\partial x} (\varphi_k + \gamma_{n_k}) \right). \quad (34)$$

We develop an iterative solution method of the time-dependent QDD model by constructing a Gummel map [21] with a set of unknown variables  $\varphi$ ,  $u$ , and  $n$  as follows:

(P1) Let  $\varphi_k^m, n_k^m$  are given, solve the nonlinear Poisson equation with respect to the electrostatic potential  $\varphi_k^{m+1}$ .  $m$  is the iteration counter. (32) is linearized using a Newton method because the potential  $\varphi$  has the strong nonlinearity. Then the linearized equation becomes

$$\lambda^2 \frac{d^2}{dx^2} \varphi_k^{m+1} - n_k^m \varphi_k^{m+1} = n_k^m - C - n_k^m \varphi_k^m. \quad (35)$$

(P2) Let  $\varphi_k^{m+1}, \varphi_{n_k}^m, S_k^m$  are given. From the linearization of (33), we obtain

$$\begin{aligned} b_n \frac{d}{dx} \left( S_k^m \frac{d}{dx} u_k^{m+1} \right) - S_k^m u_k^{m+1} \\ = -\frac{S_k^m}{2} (\varphi_k^{m+1} - \varphi_{n_k}^m). \end{aligned} \quad (36)$$

By solving (36) with respect to the variable  $u$ , we calculate  $u_k^{m+1}$  and then setting the quantum potential

$$\gamma_{n_k}^{m+1} = 2u_k^{m+1} + \varphi_{n_k}^m - \varphi_k^{m+1}. \quad (37)$$

(P3) Let  $n_{k-1}, \varphi_k^{m+1}, \gamma_{n_k}^{m+1}$  are given, solve for the electron density  $n_k^{m+1}$ . We obtain  $n_k^{m+1}$  by solving the linearized current continuity equation

$$\begin{aligned} & \frac{1}{\tau_k} (n_k^{m+1} - n_{k-1}) \\ &= \frac{\partial}{\partial x} \left( \mu_n \frac{\partial n_k^{m+1}}{\partial x} - \mu_n n_k^{m+1} \frac{\partial}{\partial x} (\varphi_k^{m+1} + \gamma_{n_k}^{m+1}) \right). \end{aligned} \quad (38)$$

We set the generalized chemical potential by

$$\varphi_{n_k}^{m+1} = \varphi_k^{m+1} + \gamma_{n_k}^{m+1} - \log n_k^{m+1}. \quad (39)$$

Here, the boundary conditions for each subproblem are the same as (22)–(25), respectively.

For space discretization, the computational domain is divided into  $M$  cells centered at  $\{x_i\}$ . The set of locations  $x_{i-1/2}$  are the positions of the interfaces bounding the computational cell. The cell sizes are given by  $h_i = x_i - x_{i-1}$ ,  $i = 1, \dots, M + 1$ . The standard scheme is applied to discretize the Poisson equation.

$$\begin{aligned} & -\lambda^2 \left( \frac{\varphi_{k,i+1} - \varphi_{k,i}}{h_{i+1}} - \frac{\varphi_{k,i} - \varphi_{k,i-1}}{h_i} \right) + n_{k,i} \varphi_{k,i} \frac{h_i + h_{i+1}}{2} \\ &= -(n_{k,i} - C) + n_{k,i} \varphi_{k,i} \frac{h_i + h_{i+1}}{2}. \end{aligned} \quad (40)$$

Space discretization of (33) is performed following our previous work [6] to achieve a high-accuracy nonlinear scheme. Assuming that the flux  $F = S \frac{du}{dx}$ , we integrate (36) with respect to  $x$  from  $x_{i-1/2}$  to  $x_{i+1/2}$ . As a result we obtain the relation

$$\begin{aligned} & \int_{x_{i-1/2}}^{x_{i+1/2}} b_n \frac{d}{dx} F dx - \int_{x_{i-1/2}}^{x_{i+1/2}} S u dx \\ &= -\frac{1}{2} \int_{x_{i-1/2}}^{x_{i+1/2}} S (\varphi - \varphi_n) dx. \end{aligned} \quad (41)$$

The flux  $F$  is defined at interfaces and then we obtain a discrete form

$$\begin{aligned} & b_n (F_{k,i+1/2} - F_{k,i-1/2}) - u_{k,i} \int_{x_{i-1/2}}^{x_{i+1/2}} S dx \\ &= -\frac{1}{2} (\varphi_{k,i} - \varphi_{n_k,i}) \int_{x_{i-1/2}}^{x_{i+1/2}} S dx. \end{aligned} \quad (42)$$

In order to find  $F_{i+1/2}$  at interfaces, integrating the flux  $F$  over the interval  $[x_i, x_{i+1}]$ , an average flux  $F_{k,i+1/2}$  yields

$$F_{k,i+1/2} = \frac{u_{k,i+1} - u_{k,i}}{\int_{x_i}^{x_{i+1}} \frac{1}{S} dx}. \quad (43)$$

A similar expression is obtained for  $F_{k,i-1/2}$ . Substituting in (42) the average fluxes, we obtain a class of conservative schemes, which was first proposed by Tikhonov and Samarskii [22]. The accuracy of the numerical flux depends on the explicit integration of  $\int_{x_i}^{x_{i+1}} \frac{dx}{S}$  in (43) and hence the explicit integration method for the function  $e^u$  leads to a procedure that produces some nonlinear schemes.

The piecewise constant representation of the potential  $u$  on the interval  $[x_i, x_{i+1}]$  leads to an average flux

$$F_{k,i+1/2} = \frac{\sqrt{n_i}}{h_{i+1}} \exp\left(\frac{u_{k,i+1} + u_{k,i}}{2}\right) \times (u_{k,i+1} - u_{k,i}). \quad (44)$$

As shown in [6], this discrete form yields the numerical flux derived by Ancona in [8]. In fact, if the unknown variable  $S$  is used, it is easy to check that

$$\begin{aligned} F_{k,i+1/2} &= \frac{1}{h_{i+1}} \sqrt{\frac{S_{k,i+1}}{S_{k,i}}} \\ &\times B\left(\ln\left(\frac{S_{k,i+1}}{S_{k,i}}\right)\right) \cdot (S_{k,i+1} - S_{k,i}) \end{aligned} \quad (45)$$

$$= \frac{1}{h_{i+1}} \frac{\sqrt{\frac{S_{k,i+1}}{S_{k,i}}}}{\frac{S_{k,i+1}}{S_{k,i}} - 1} \ln\left(\frac{S_{k,i+1}}{S_{k,i}}\right) \cdot (S_{k,i+1} - S_{k,i}). \quad (46)$$

In order to construct a higher-accuracy nonlinear scheme, an explicit integration of  $e^u$  is obtained by the piecewise linear approximation of  $u$  on the interval  $[x_i, x_{i+1}]$ . Then we have

$$\int_{x_i}^{x_{i+1}} e^{-u} dx = \frac{1}{\sqrt{n_i}} \frac{h_{i+1} e^{-u_{k,i+1}}}{B(u_{k,i+1} - u_{k,i})} \quad (47)$$

where  $B(x) = \frac{x}{e^x - 1}$  is the Bernoulli function. Substituting (47) into (43) results in the numerical flux introduced by Odanaka in [6]:

$$F_{k,i+1/2} = \frac{\sqrt{n_i}}{h_{i+1}} e^{u_{i+1}} B(u_{k,i+1} - u_{k,i})(u_{k,i+1} - u_{k,i}). \quad (48)$$

A similar expression is obtained for  $F_{k,i-1/2}$ . An average of  $S$  in each computational cell is obtained by integrating the piecewise-linear representation of  $u$  on the interval  $[x_{i-1/2}, x_{i+1/2}]$ . Then we have

$$\begin{aligned} \Lambda_{k,i} &= \int_{x_{i-1/2}}^{x_{i+1/2}} S dx \\ &= \sqrt{n_i} \left( \frac{h_i e^{u_{k,i}}}{2B(\frac{u_{k,i-1} - u_{k,i}}{2})} + \frac{h_{i+1} e^{u_{k,i}}}{2B(\frac{u_{k,i+1} - u_{k,i}}{2})} \right). \end{aligned} \quad (49)$$

Substituting (48) and (49) into (42) leads to a high-accuracy nonlinear scheme introduced in [6].

$$\begin{aligned} &\sqrt{n_i} b_n \left( \frac{1}{h_{i+1}} e^{u_{k,i+1}} B(u_{k,i+1} - u_{k,i})(u_{k,i+1} - u_{k,i}) \right. \\ &\quad \left. - \frac{1}{h_i} e^{u_{k,i}} B(u_{k,i} - u_{k,i-1})(u_{k,i} - u_{k,i-1}) \right) - \Lambda_{k,i} u_{k,i} \\ &= -\frac{\varphi_{k,i} - \varphi_{n,k,i}}{2} \Lambda_{k,i}. \end{aligned} \quad (50)$$

This scheme results in a consistent generalization of the Scharfetter-Gummel expression [23] to the Sturm-Liouville type equation [6].

For space discretization of the current continuity equation, (34) is rewritten in terms of the Slotboom variables  $\eta = n_i \exp(-\varphi_n)$  for the generalized chemical potential as

$$\frac{1}{\tau_k} (n_k - n_{k-1}) = \operatorname{div}(\mu_n e^{\Phi_k} \nabla \eta_k) \quad (51)$$

where  $\Phi_k = \varphi_k + \gamma_{n,k}$ .  $\tau_k$  denotes the time step for  $k = 1, \dots, N$ . The current density  $J_n = \mu_n e^\Phi \nabla \eta$  is discretized in terms of the electron density, then we obtain

$$J_{n_{i+1/2}} = \mu_{n_{i+1/2}} \frac{\eta_{k,i+1} - \eta_{k,i}}{\int_{x_i}^{x_{i+1}} e^{-\Phi_k} dx} \quad (52)$$

$$\begin{aligned} &= \frac{\mu_{n_{i+1/2}}}{h_{i+1}} (B(\Phi_{k,i+1} - \Phi_{k,i}) n_{k,i+1} - B(\Phi_{k,i} \\ &\quad - \Phi_{k,i+1}) n_{k,i}). \end{aligned} \quad (53)$$

As a result, the well-known Scharfetter-Gummel scheme [23] to (34) is derived as

$$\begin{aligned} &\frac{1}{\tau_k} (n_{k,i} - n_{k-1,i}) \\ &= \frac{\mu_{n_{i+1/2}}}{h_{i+1}} (B(\Phi_{k,i+1} - \Phi_{k,i}) n_{k,i+1} \\ &\quad - B(\Phi_{k,i} - \Phi_{k,i+1}) n_{k,i}) \\ &\quad - \frac{\mu_{n_{i-1/2}}}{h_i} (B(\Phi_{k,i} - \Phi_{k,i-1}) n_{k,i} \\ &\quad - B(\Phi_{k,i-1} - \Phi_{k,i}) n_{k,i-1}). \end{aligned} \quad (54)$$

## 5 Adaptive time step control

An effective way for the time step control is to look at the ratio of consecutive gradients of the free energy, i.e.,

$$\theta = \frac{W_{k+1} - W_k}{W_k - W_{k-1}} = \frac{\int_{t_k}^{t_{k+1}} H(t) dt}{\int_{t_{k-1}}^{t_k} H(t) dt}, \quad (55)$$

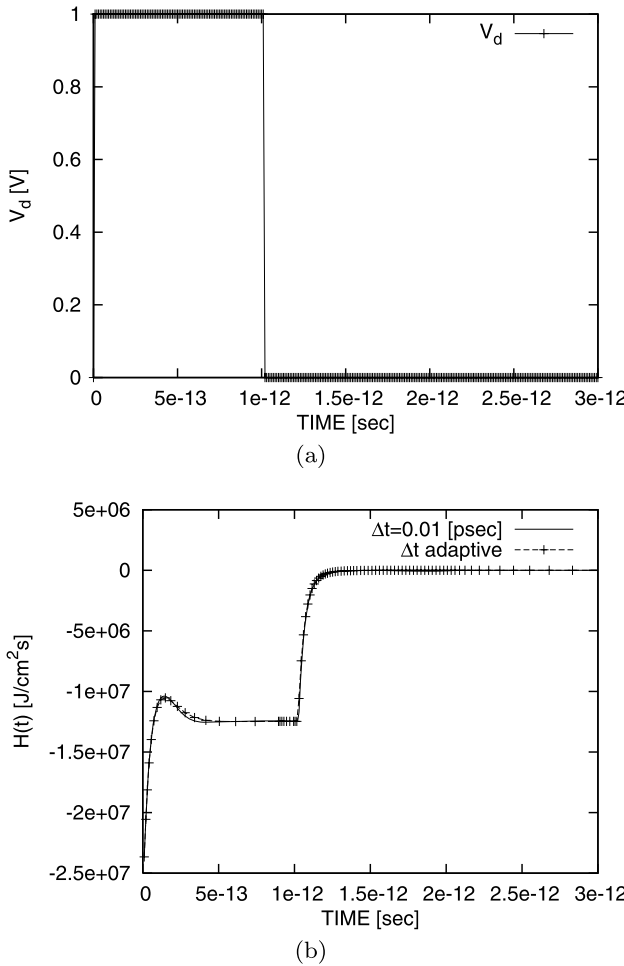


**Fig. 3** A comparison of the derivatives of free energy after an abrupt fall of input voltage. The result calculated by the adaptive time step is compared with the “exact” solution obtained from the fine time step of 0.01 psec. (a) A waveform of the input voltage. (b) The derivatives of free energy as a function of time

where  $W_k = \int_0^{t_k} H(t)dt$ . If the value of  $\theta$  is near 1 then the system approaches the stationary state and hence the time step size can be increased. If  $\theta$  is far from 1, then the free energy of the system is greatly changed in time and hence the step size is kept to be constant. Using the value of  $\theta$ , an adaptive time step algorithm is constructed as follows:

$$\tau_{k+1} = \alpha(\theta)\tau_k, \quad (56)$$

$$\alpha(\theta) = \begin{cases} 1.2 & |\theta - 1| < d_{min}, \\ 1.0 & d_{min} \leq |\theta - 1| \leq d_{max}, \end{cases} \quad (57)$$

where  $d_{min}$  and  $d_{max}$  are parameters. In this work,  $d_{min} = 0.2$ , and  $d_{max} = 0.5$ . When  $d_{max} < |\theta - 1|$ , the solution at  $t = t_k$  is re-calculated as

$$\tau_k = \tau_{min}, \quad \text{if } d_{max} < |\theta - 1|, \quad (58)$$

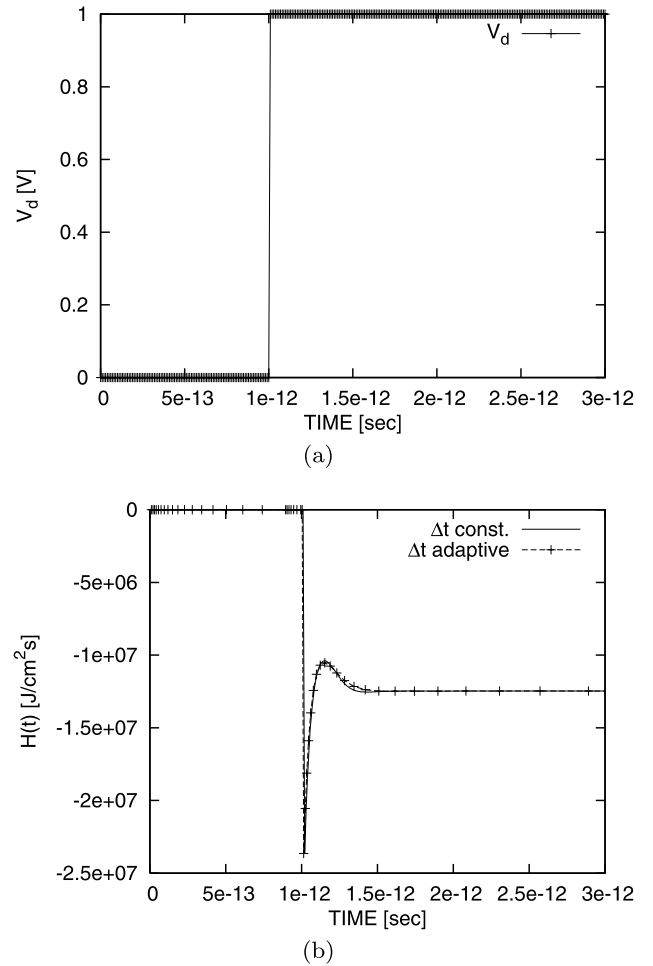


**Fig. 4** A comparison of the derivatives of free energy after an abrupt rise of input voltage. The result calculated by the adaptive time step is compared with the “exact” solution. (a) A waveform of the input voltage. (b) The derivatives of free energy as a function of time

where  $\tau_{min}$  is the minimum time step. In order to calculate the value of  $\theta$  in (55),  $H(t)$  is approximated by the second degree Lagrange interpolating polynomial  $P(t)$ .  $P(t)$  is obtained as

$$P(t) = a_{k-2} + a_{k-1}(t - t_{k-2}) + a_k(t - t_{k-2})(t - t_{k-1}), \quad (59)$$

$$a_{k-2} = P(t_{k-2}) = H_{k-2}, \quad (60)$$

$$a_{k-1} = H(t_{k-2}, t_{k-1}) = \frac{H_{k-1} - H_{k-2}}{t_{k-1} - t_{k-2}}, \quad (61)$$

$$a_k = H(t_{k-2}, t_{k-1}, t_k) = \frac{H(t_{k-1}, t_k) - H(t_{k-2}, t_{k-1})}{t_k - t_{k-1}} \\ = \frac{\frac{H_k - H_{k-1}}{t_k - t_{k-1}} - \frac{H_{k-1} - H_{k-2}}{t_{k-1} - t_{k-2}}}{t_k - t_{k-2}}. \quad (62)$$

As  $\tau_{k+1} = \tau_k$ ,  $\theta$  at  $t = t_{k+1}$  is predicted by integrating  $P(t)$  in (55). Then  $\alpha(\theta)$  is estimated in (57) using the value of  $\theta$ .

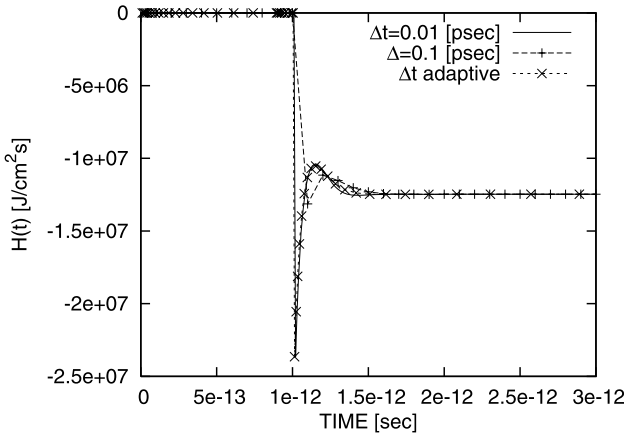


**Fig. 5** A comparison of the derivatives of free energy calculated by the fine time step of 0.01 psec and large time step of 0.1 psec

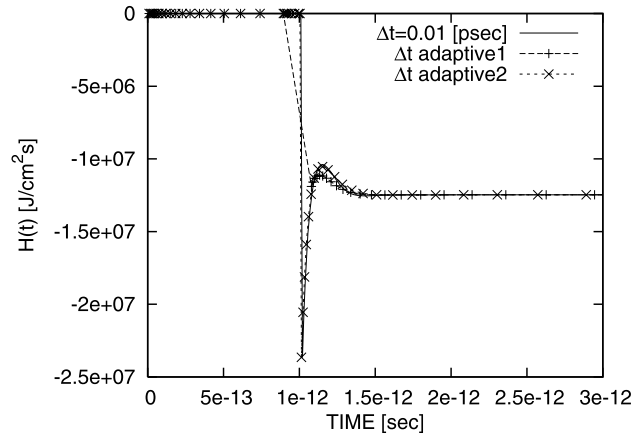


**Fig. 7** A comparison of the derivatives of free energy calculated by the adaptive time step algorithms with and without the re-calculation procedure of time step

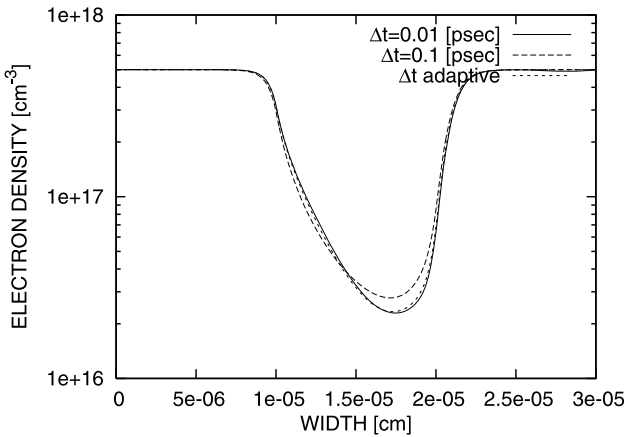


**Fig. 6** Electron density distributions after an abrupt rise of input voltage. The results calculated by the large constant time step and the adaptive time step control are compared with the “exact” solution

Using (56), the next time step  $\tau_{k+1}$  is corrected. In the work the minimum time step is set up to be 0.01 psec.

## 6 Numerical results

The resulting algorithm was verified with the switching characteristics of an n<sup>+</sup>-n-n<sup>+</sup> silicon diode having  $5 \times 10^{17}$  cm<sup>-3</sup> and  $2 \times 10^{15}$  cm<sup>-3</sup> at room temperature. The channel length  $l$  is 0.1  $\mu$ m. When the drain voltage is applied, the n<sup>+</sup>-n-n<sup>+</sup> diode is on. In the discussion of switching characteristics, therefore, the input waveform is when the drain voltage makes an abrupt transition from high to low or vice versa.

Figure 3 shows the derivatives of the free energy of the system as a function of time. In this case, the drain voltage makes an abrupt transition from 1.0 V to 0.0 V, shown in Fig. 3(a). The adaptive time step algorithm represents the

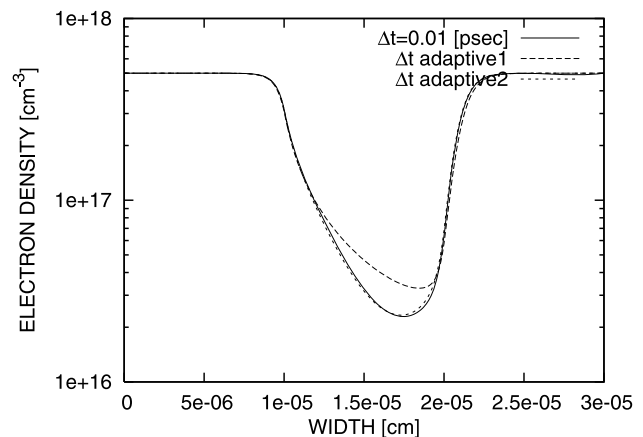


**Fig. 8** Electron density distributions after an abrupt rise of input voltage. The results calculated by the adaptive time step algorithms with and without the re-calculation procedure of time step are compared with the “exact” solution

“exact” solution obtained from the fine constant time step of 0.01 psec, as shown in Fig. 3(b). Figure 4 compares the derivatives of free energy between the fine time step control and the new algorithm. The waveform of the input voltage from 0.0 V to 1.0 V is shown in Fig. 4(a). The result also confirms in Fig. 4(b) that the new algorithm represents the exact solution calculated by the fine time step after an abrupt rise of input voltage.

The result for the large constant time step control is shown in Fig. 5. The large constant time step of 0.1 psec, however, can not accurately calculate the derivative of free energy during the step transition. As shown in Fig. 6, this causes the large discrepancy of electron density distributions after the abrupt rise of input voltage. It is found that the proposed algorithm gives a good approximation to the electron density distribution.

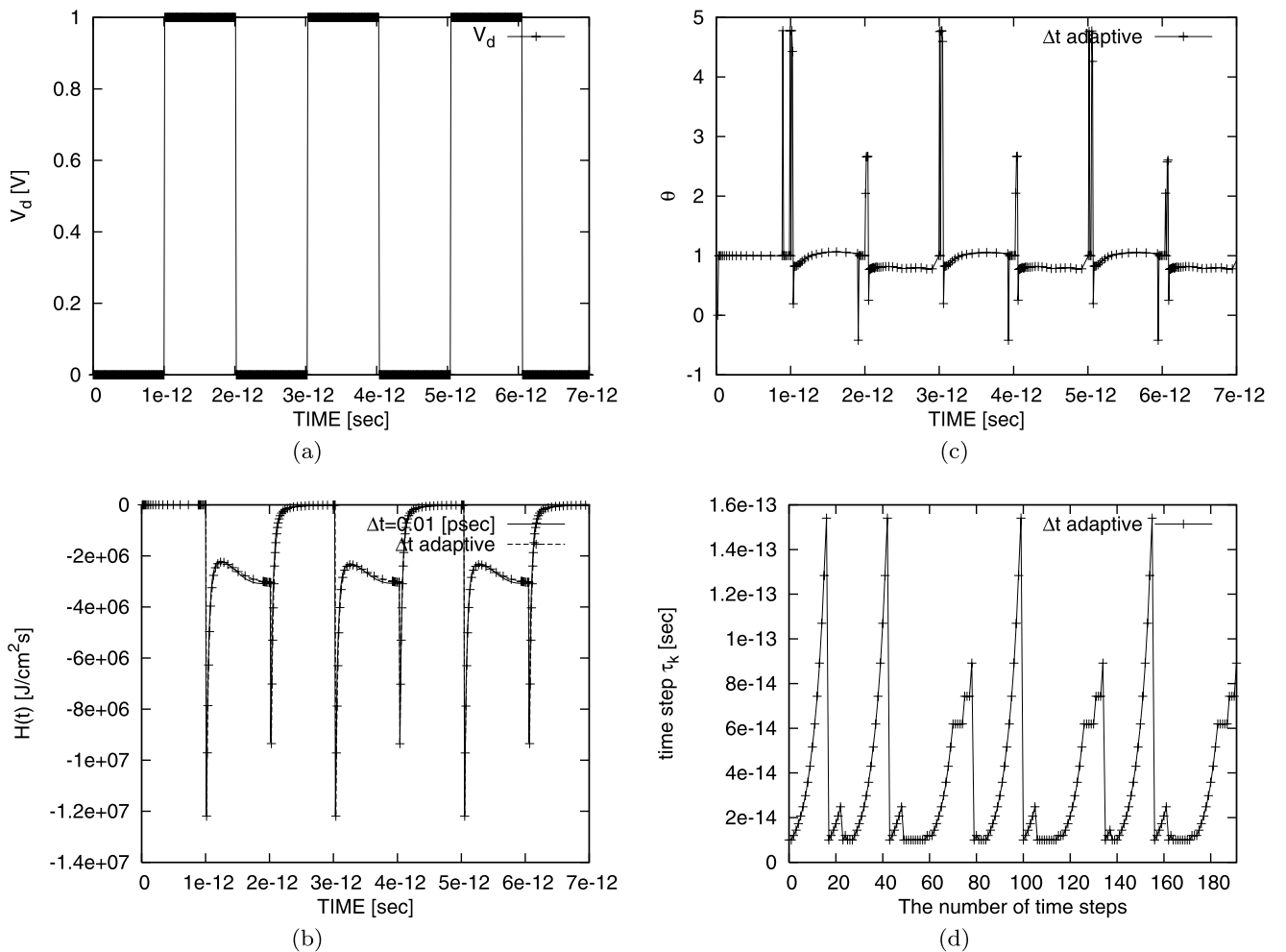


**Fig. 9** Evolution of time step for switching characteristics of an  $n^+-n-n^+$  device with  $l = 0.2 \mu\text{m}$ . (a) Input waveform. (b) The derivative of free energy as a function of time. (c) The value of  $\theta$  as a function of time. (d) Evolution of adaptive time step

When the drain voltage is kept to be 0 V before the transition, the  $n^+-n-n^+$  diode approaches the thermal equilibrium and hence the time step increases. After the drain voltage  $V_d$  switches from 0 V to 1.0 V, the fine time step is needed, since the system behavior is greatly changed. If the re-calculation procedure of time step (58) is implemented into the adaptive time step algorithm, the timestep is adapted before the step transition. Figure 7 compares the derivatives of free energy calculated by two algorithms with and without the re-calculation procedure of time step. Before the abrupt rise of input voltage the fine time step is generated according the re-calculation procedure of time step and hence the time step is adapted to the abrupt transition. As a result, as shown in Fig. 8, there is a significant difference of electron density distributions between two algorithms.

Figure 9 shows the evolutions of time step for the full switching characteristics of an  $n^+-n-n^+$  device with  $l = 0.2 \mu\text{m}$ , with respect to the input waveform shown in Fig. 9(a). In Fig. 9(b), the derivatives of free energy as a

function of time are compared with the “exact” solution. The time step is controlled by the value of  $\theta$  shown in Fig. 9(c) predicting the derivatives of free energy of the system. The evolution of time step is shown in Fig. 9(d). The result indicates that the time step is adapted to the switching characteristics. The total number of time steps is significantly decreased with the new algorithm.

## 7 Conclusion

A numerical method for a transient QDD model has been proposed with emphasis on adaptive time discretization. The adaptive time step algorithm for the transient QDD model is constructed by predicting the derivative of the free energy of the system, which is the same form as that of the classical DD model by using the generalized chemical potential. It was shown that the time step is adapted to the switching characteristics of  $n^+-n-n^+$  diodes. The new algorithm significantly reduces the total number of time step.

**Acknowledgements** The authors thank Professors A. Matsumura of Osaka University and A. Hiroki of Kyoto Institute of Technology for valuable discussions.

## References

1. Ancona, M.G., Iafrate, G.J.: Quantum correction to the equation of state of an electron gas in a semiconductor. *Phys. Rev. B* **39**, 9536–9540 (1989)
2. Gardner, C.L.: The quantum hydrodynamic model for semiconductor devices. *SIAM J. Appl. Math.* **54**, 409–427 (1994)
3. Rafferty, C.S., Biegel, B., Yu, Z., Ancona, M.G., Bude, J., Dutton, R.W.: Multi-dimensional quantum effect simulation using a density-gradient model and script-level programming techniques. In: Proc. SISPAD, pp. 137–140 (1998)
4. Ancona, M.G., Yu, Z., Dutton, R.W., Vande Voorde, P.J., Cao, M., Vook, V.: Density-gradient analysis of MOS tunneling. *IEEE Trans. Electron. Dev.* **47**, 2310–2319 (2000)
5. Pinnau, R., Unterreiter, A.: The stationary current-voltage characteristics of the quantum drift-diffusion model. *SIAM J. Numer. Anal.* **37**, 211–245 (1999)
6. Odanaka, S.: Multidimensional discretization of the stationary quantum drift-diffusion model for ultrasmall MOSFET structures. *IEEE Trans. Comput. Aided Des. Integr. Circuits Syst.* **23**, 837–842 (2004)
7. de Falco, C., Gatti, E., Lacaita, A.L., Sacco, R.: Quantum-corrected drift-diffusion models for transport in semiconductor devices. *J. Comput. Phys.* **204**, 533–561 (2005)
8. Ancona, M.G.: Finite-difference schemes for the density gradient equations. *J. Comput. Electron.* **1**, 435–443 (2002)
9. Odanaka, S.: A high-resolution method for quantum confinement transport simulations in MOSFETs. *IEEE Trans. Comput. Aided Des. Integr. Circuits Syst.* **26**, 80–85 (2007)
10. Pinnau, R.: Numerical approximation of the transient quantum drift diffusion model. *Nonlinear Anal.* **47**, 5849–5860 (2001)
11. Ferry, D.K., Zhou, J.-R.: Form of the quantum potential for use in hydrodynamic equations for semiconductor device modeling. *Phys. Rev. B* **48**, 7944–7950 (1993)
12. Jüngel, A., Pinnau, R.: A positivity-preserving numerical scheme for a nonlinear fourth order parabolic system. *SIAM J. Numer. Anal.* 385–406 (2001)
13. Ancona, M.G., Tiersten, H.F.: Macroscopic physics of the silicon inversion layer. *Phys. Rev. B* **35**, 7959–7965 (1987)
14. Jüngel, A., Pinnau, R.: Global non-negative solutions of a nonlinear fourth-order parabolic equation for quantum systems. *SIAM J. Math. Anal.* **32**, 760–777 (2000)
15. Brezzi, F., Gasser, I., Markowich, P.A., Schmeiser, C.: Thermal equilibrium states of the quantum hydrodynamic model for semiconductors in one dimension. *Appl. Math. Lett.* **8**, 47–52 (1995)
16. Mock, M.S.: *Analysis of Mathematical Models of Semiconductor Devices*. Boole Press, Dublin (1983)
17. Gajewski, H., Gröger, K.: On the basic equations for carrier transport in semiconductors. *J. Math. Anal. Appl.* **113**, 12–35 (1986)
18. Gajewski, H., Kaiser, H.-C., Langmach, H., Nürnberg, R., Richter, R.H.: Mathematical modelling and numerical simulation of semiconductor detectors. In: Jäger, W., Krebs, H.-J. (eds.) *MATHEMATICS—Key Technology for the Future*, pp. 355–364. Springer, Berlin (2003)
19. Shimada, T., Odanaka, S.: Adaptive time discretization for a transient quantum drift-diffusion model. In: Proc. SISPAD, pp. 337–340 (2007)
20. Unterreiter, A.: The thermal equilibrium solution of a generic bipolar quantum hydrodynamic model. *Commun. Math. Phys.* **188**, 69–88 (1997)
21. Gummel, H.K.: A self-consistent iterative scheme for one-dimensional steady state transistor calculations. *IEEE Trans. Electron Dev.* **11**, 455–465 (1964)
22. Marchuk, G.I.: *Methods of Numerical Mathematics*. Springer, Berlin (1982)
23. Scharfetter, D., Gummel, H.K.: Large signal analysis of a silicon Read diode oscillator, 16, 64–77 (1969)